First-Principles Study of Solar Cell Power Conversion Efficiency of Organic Molecules

Mary Catlett, Dr. Mario F. Borunda

Contents

First-Principles Study of Solar Cell Power Conversion Efficiency
of Organic Molecules

Mary Catlett, Dr. Mario F. Borunda

Abstract

We present our first-principles studies on the power conversion efficiency (PCE) of organic molecules. Usually, molecular materials have a low PCE for solar cell applications. Using computational screening methods can point out families of molecules that might be good candidates for photovoltaics. In this study, we use experimental data on a set of organic molecules to compare a theoretical method for predicting PCE, first proposed by Scharber, and computations of the optical absorption of the molecules.

The Scharber model predicts the PCE from the energy levels of the molecule. Our approach uses time-dependent Density Functional Theory (TD-DFT) to calculate the optical absorption which is then integrated for a prediction of the PCE. The molecular set was chosen from systems where PCE experimental data is available from the literature, thus, we can then compare the predictive power of the calculations.

First-Principles Study of Solar Cell Power Conversion Efficiency of Organic Molecules

Mary Catlett, Dr. Mario F. Borunda

Broader Impact

Organic molecules make ideal photovoltaic materials due to their inexpensive and environmentally friendly manufacturing process. Certain molecules reached a 17% Power Conversion Efficiency (PCE) September 2018 [1], making them competitive with already commercialized silicon based solar cells, if scientists can continue finding high performing organics. The experimental search for other molecules with a high enough PCEs can be aided by theoretical methods. The Scharber model is used to predict the PCE of a set of molecules to prioritize ones for experiment [2-3]. The model uses the energy of the highest occupied molecular orbital (HOMO) and that of the lowest unoccupied molecular orbital (LUMO) and the same values for fullerenes derivatives and assumes a quantum yield to predict the compound's PCE.

A sample graph of this model is shown below:

In this ongoing study, we want to find the Quantum Yield (QY) for each molecule using the overlap between the solar spectrum and the optical absorption obtained from TD-DFT [4-5] calculations. The molecules in this study were chosen for their

semiconducting properties and available literature on electronic properties [6-17]. In the
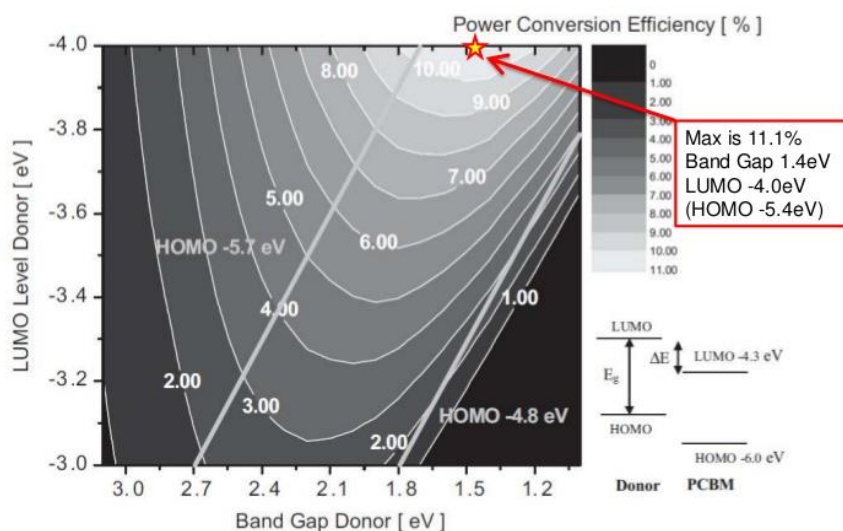
future, we will investigate the accuracy this calculated quantum yield predicts molecular PCE's in comparison to the Scharber Model.

This project, when completed, will aid the broader community of materials researchers searching for high performing organic photovoltaics. By comparing the accuracy of the Scharber Model to DFT and our own revisions to the Scharber Model, we will be able to communicate to the scientific community which method works the best.

**First-Principles Study of Solar Cell Power Conversion Efficiency
of Organic Molecules**

Mary Catlett, Dr. Mario F. Borunda

Methodology

From 12 different published articles [6-17], we found 32 semi-conductive molecules to base our study on. We chose them because of the published data on their absorption spectrums and photo-electric properties. Then we compared the published data to what our theory generated. This method of comparing quantum theory to already published data is very similar to the methods of Zhang and Musgrave [18]. An outline of our specific methods for this project are shown by the figure below, with the number of molecules in stages 4 and 5 indicated:
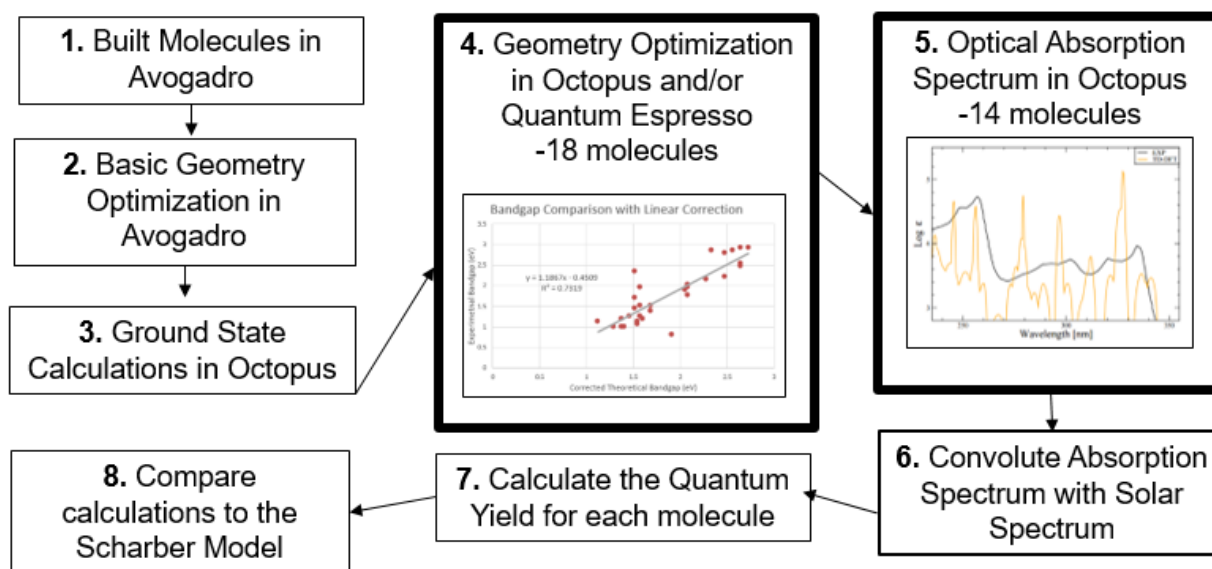
First, we manually constructed a model of each molecule from the papers in Avogadro [19]. We used the "optimize geometry" feature to optimize the molecule's structure using molecular mechanics. Using the simple calculation was only a first step, because the math used by Avogadro to obtain the "optimize geometry" was not detailed enough for our project.

However, it did generate values in the general vicinity of the one we needed. This step was a way to reduce the amount of time for subsequent calculations.

Our next step was to transfer our coordinates to the Octopus software suite [20]. This software uses a simulation box of specified size to simulate the quantum properties of the molecule being modeled. It does so by sampling a discrete set of points throughout the system as a mesh of specified spacing. We needed to optimize the box-size and calculation spacing before continuing the simulations. Doing so prevents our results from distorting to a molecule shape that does not behave like reality. We chose the smallest molecule $(C_{10}H_6S_2)_8$ in our data set, shown in figure below, to optimize the parameters because it took the least amount of computing time.

At first, we thought we could optimize the calculation spacing before the box size. However, the energy values of the system did not converge for parts of the test simulations. This led us to take the opposite approach.

We next tried to see how the molecule interacted with itself in 3 dimensions with the set the mesh spacing of 0.2 Angstroms (Å). We chose that calculation spacing because it did not take too much computation time when used in an iteration of the previous study. It is generally assumed for these studies that the larger the box size, the more accurate the calculations. However, when the box gets to be too large, the calculation fails to complete. So, we chose to double the x and y dimensions from their minimum values. Then we decided to optimize the z direction because of its initial size of 0 Å. The z value was then increased incrementally for each calculation from 1 to 10 Å. We chose the optimal added x, y, and z dimensions to be 5, 3, and 6 Å respectively based on where the system energy converged for the iterations. We could have

taken the time to further optimize the x and y dimensions. We did not because based on our energy convergence data, further optimization would not significantly affect the outcome of our calculation. The purpose of these parameter optimizations was to get something repeatedly working with minimal computing time, which was accomplished. For all further calculations, we added those dimensional values to the minimum system size for each molecule. Errors did come up later when molecular orbitals were expanded past the system size. For those molecules, we added extra spacing, 1 to 2 Å at a time until the system size included those orbitals.

We then returned to our attempt at optimizing the calculation mesh spacing with our optimized box size. The study converged between 0.15 and 0.2 Å. This meant that our optimal spacing range was 0.15 to 0.2 Å. We chose to use 0.15 Å as the spacing for the rest of the project so we could have the freedom to adjust to 0.2 Å as needed. Adjustments to 0.2 Å were made when a molecule system was taking too much time to complete. This increase led to decreased computing time without losing significant accuracy. The data from this study was also used to justify a spacing increase to 0.25 Å for a few of the largest molecules. Notes of these changes were also kept as they came about. Graphs of these optimization studies are shown below:

Box Study

ΔE (Ry) vs Lz (Å)

Spacing Study 2

ΔE (Ry) vs Spacing (Å)
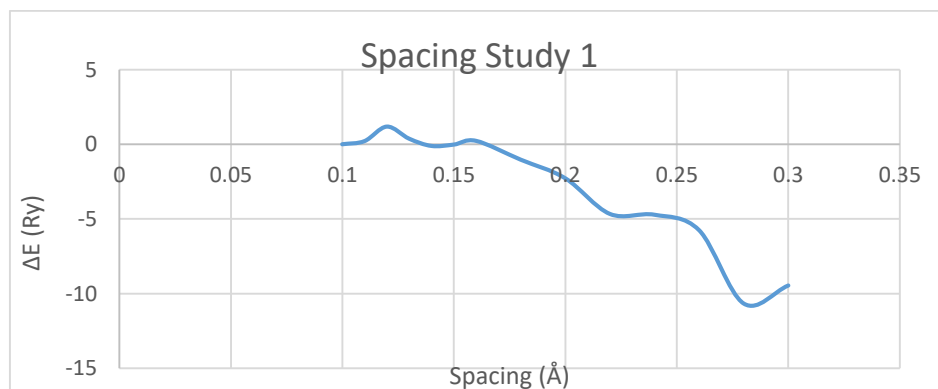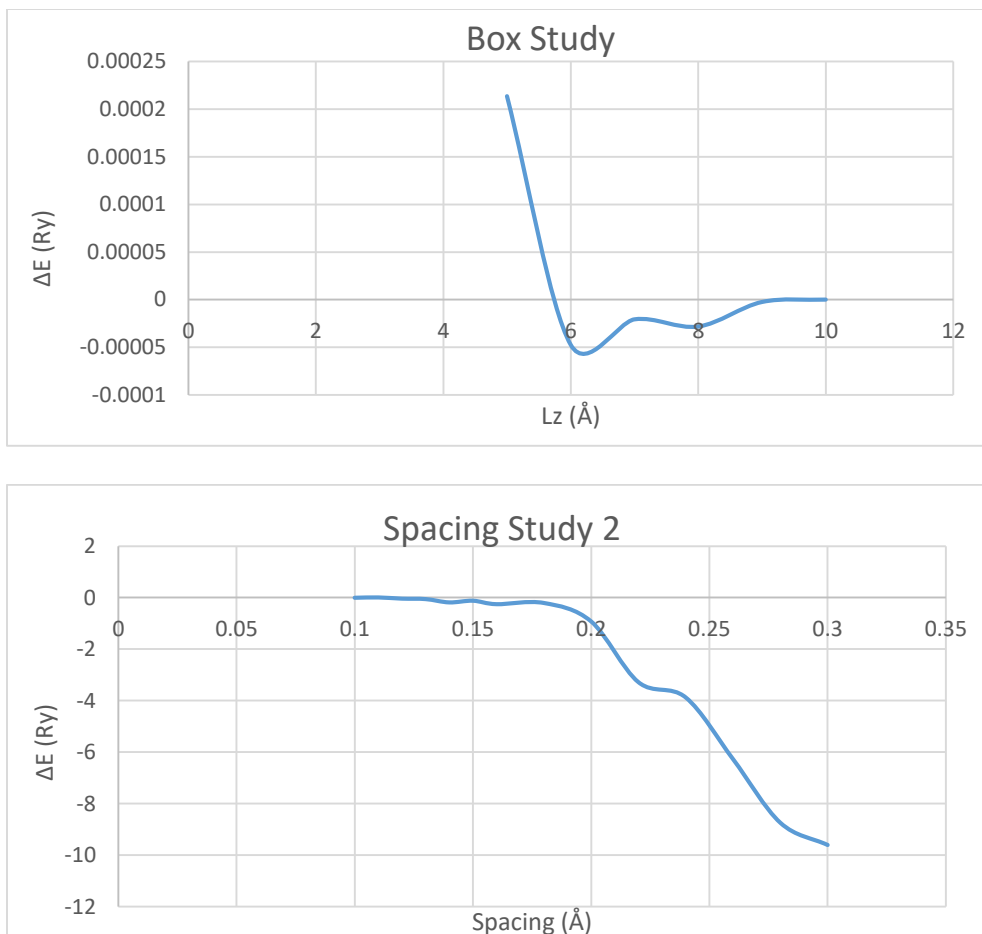
The next step in optimization was to calculate the ground state energies of the molecule. Octopus has a special mode for this that we used. The time for these calculations ranged from 5 hours to 5 days for each molecule. We knew the calculation was completed based on the default criteria of the program. For each molecule, it took between 2 to 4 attempts to complete a calculation due to the user's learning curve for proper operation.

From the ground state calculation, we could calculate an optimized geometry in Octopus. Although we did calculate an optimized geometry in Avogadro previously, continuing the calculation in Octopus allowed us to get a calculation that accounted for the molecules quantum properties. This was a very important part of the optimizations because we tried to bring our simulation as close to reality as possible. After each calculation, we checked the maximum forces

and energy gap values of the molecule to see if the calculation was complete. For the energy gaps, we were looking for consistency instead of an exact match to data. This was because the DFT version, Local Density Approximation (LDA) we used is known to consistently underestimate [21]. We used it for our optimization calculations despite of this because of its low computation time. Since this part of the project was only an optimization phase, we decided to leave the more computationally intensive calculations for the final phase of the project. For our DFT exchange functional, we used Purdue Zunger (PZ) because of the pre-generated pseudopotentials available for us to use. The decision to continue iterations was based on the maximum force value. We concluded that the geometry was optimized when the molecules maximum bond forces reached 0.01 eV/ Å. However, after 2 years of submitting calculations, only 5 of the molecules reached these convergence criteria.

Due to time consuming flaws in the Octopus software system, we switched to the Quantum Espresso software suite [22] to complete the geometry optimizations. We also added a parallel computing function to our submission script to decrease our calculation times. We took the most recent iteration of the Octopus geometry optimization for each molecule and resubmitted it using Quantum Espresso.

The optimization of the Quantum Espresso geometry optimization mode was not specifically done for this project. Instead, optimized system sizes were borrowed from studies done on previous project molecules. For this project, there were some studies done to explore the appropriate amount of computing hardware to be used based on the size of each molecule system. The results of that led to us splitting the molecules into two sets based on size. The calculations for the set of larger molecules were done on the supercomputing nodes with more

memory space than the nodes used for the set of smaller molecules. Currently, we are in the process of implementing this method before we move on to the next steps of our project.

We will next take the optimized geometries for each molecule to calculate their respective absorption spectrums. We will use Time Dependent Density Functional Theory (TD-DFT) [23] and a delta kick function in Octopus [20]. The data from this part of the project will be an absorption curve and an emission curve. These calculations will be repeated for each molecule. Each calculation is expected to take between 1 and 5 days. A graphic modeling how this calculation works is shown below:
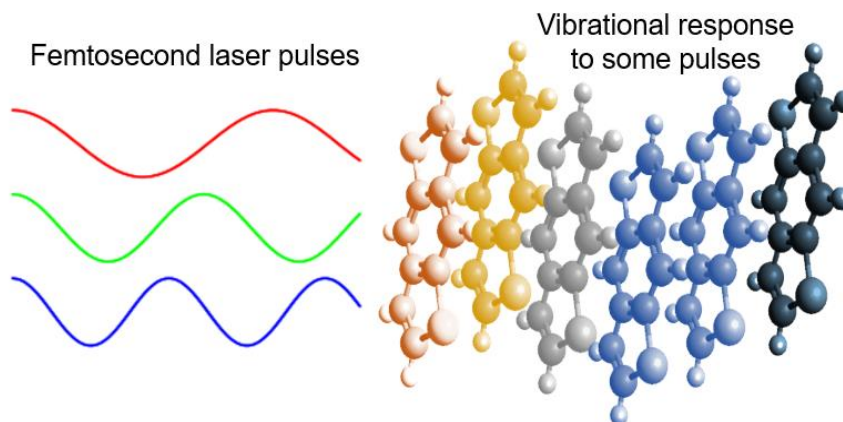
The next part of the project is to analyze the data from the absorption spectrums. First, we will integrate photo-electric curves calculated by TD-DFT to find the number of photons absorbed and emitted for each molecule. Then we will divide the number of photons emitted by the number of photons absorbed to find each molecule's quantum yield. This will be for all of the molecules. Subsequently, we will return our analysis to each molecule's absorption spectrum. We will next use Python [24] to calculate the absorption spectrum of the molecule with the emission spectrum of the sun.

Next, we will use the methods outlined in Scharber's paper to find the band gaps, quantum yield, absorption spectrum, and solar spectrum for each molecule. We will then compare the Scharber calculation theoretical values to the TD-DFT values by looking at a percent difference of the value compared to experiment.

First-Principles Study of Solar Cell Power Conversion Efficiency of Organic Molecules

Mary Catlett, Dr. Mario F. Borunda

Current Results

LUMO Comparison

$$y = 0.9808x - 0.6152$$
$$R^2 = 0.6727$$
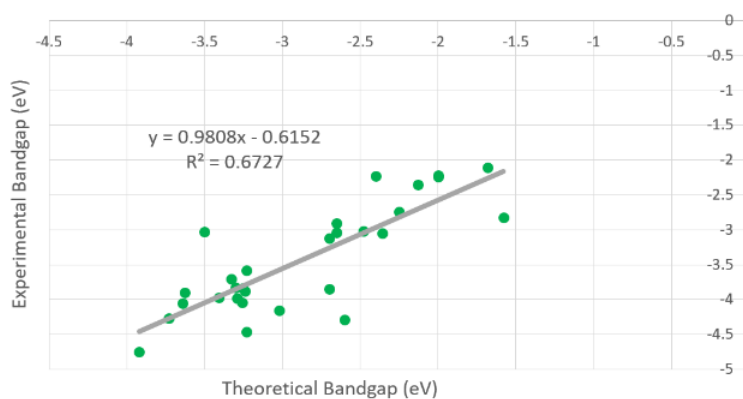
Figures 1 : LUMO Data from Octopus Geometry Optimizations

Energy Gap Comparison with Linear Correction

$$y = 1.1867x - 0.4509$$
$$R^2 = 0.7319$$
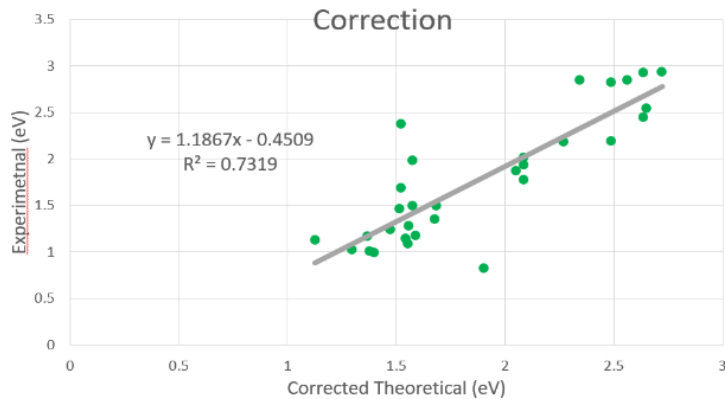
Figures 2 : Energy Gap Data from Octopus Geometry Optimizations with linear correction
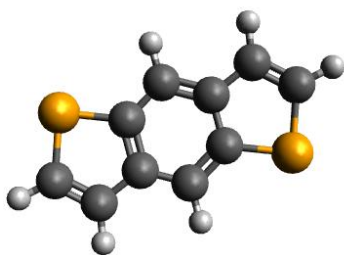
Figures 13 and 14: M5_1a molecule (above) and its theoretical and experimental optical absorption spectrums (right)
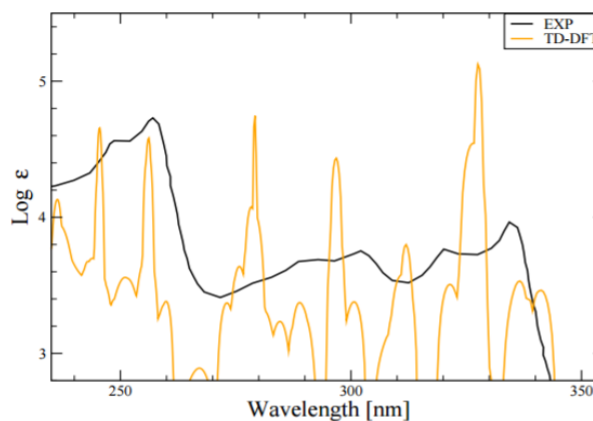
The trend of our data in Figures 1 and 2 indicate that DFT-LDA is underestimating the LUMOs and overestimating the HOMOs. Our band gap results show a linear correlation between experiment and theory, once we have applied a linear correction. This indicates that the theory is consistent in its over and underestimations. To increase the accuracy of our band gap calculations, we can further optimize our molecular geometry calculations.

In figure 13, the experimental data came from a crystal of molecules, whereas the theoretical data came from a system of one molecule. The absorption spectrum of the experimental data shows then the average energy of multiple molecules interacting in a system. That of the theoretical data shows for only one molecule. If we were to place multiple molecules in the 1a system, we might see a closer correlation between the two results. However, for the purposes of this study, we will only continue to use one molecule. For future calculations plan to decrease the oscillation discrepancy between experiment and theory by matching temperatures of the systems.

When we switched our software from Octopus to Quantum Espresso, we found that the systems for each of our molecules optimized overwhelmingly faster, as shown by the table below:

Molecule	Octopus Convergence Time	QE Convergence Time
M5_1a	~150 hours	~1 hour
M5_1b	~175 hours	~1.5 hours
M5_2b	~200 hours	~4 hours
M7	200+ hours	~17 hours
M13_a	200+ hours	~5 hours
M13_d	200+ hours	~26 hours

Factors contributing to QE being faster were that bugs in Octopus program affected units of measurement conversion and data management, the use of parallel computing when made

transition to Quantum Espresso, newer supercomputer hardware at time of transition, and the last set of coordinates from Octopus runs for each molecule was used as starting point for Quantum Espresso calculations. However, there were Similar trends between programs, such as the smallest molecules converging first and the larger molecules containing Fluorine, Sulfur, and Silicon have not yet converged.

First-Principles Study of Solar Cell Power Conversion Efficiency of Organic Molecules

Mary Catlett, Dr. Mario F. Borunda

Publication and Public Release Plans

We have publicly released stages of our project through 4 different presentations, which are attached to this document in the appendix. The list of the presentations is shown below, with links to view them on Google Docs:

1. APS Conference for Undergraduate Women in Physics| Corpus Christi, TX | January 2019
   Poster: First-Principles Study of Solar Cell Power Conversion Efficiency of Organic Molecules
   https://drive.google.com/file/d/1NYXz9ldCvFYQtr3KWZCVNVsx8yh_tun7/view?usp=sharing

2. OSU Physics Department Senior Project | Stillwater, OK | December 2018
   Oral Presentation: First-Principles Study of Solar Cell Power Conversion Efficiency of Organic Molecules
   https://drive.google.com/file/d/1Hz2ajEu2R1Tg3PODbohBYkdJ_FO7cCw3/view?usp=sharing

3. 2018 Annual Oklahoma Photovoltaic Research Institute Meeting | Stillwater, OK |
   Poster: Finding the Energy Gaps of Organic Molecules   April 2018
   https://drive.google.com/file/d/1ENHZWB83aUsaIbucpLhu6IX29gFafjEU/view?usp=sharing

4. 2016 National Meeting for SACNAS |Long Beach, CA | October 2016
   Poster: Finding the Quantum Yield of Organic Molecules with Photovoltaic Applications
   https://drive.google.com/file/d/1dCgZL0wlN8R5pP7BDY5Wt7_gm9XXCXNJ/view?usp=sharing

We also presented at the National Conference for Undergraduate Research in April 2019 and the Oklahoma Photovoltaic Research Symposium in April 2019. Once we complete our data collection this semester, we plan to prepare a manuscript for professional publication in a scientific journal. The journal we will submit will be chosen once we have completed our final data collection.

First-Principles Study of Solar Cell Power Conversion Efficiency
of Organic Molecules
Mary Catlett, Dr. Mario F. Borunda

References

1. Meng, L., Zhang, Y., Wan, X., Li, C., Zhang, X., Wang, Y., . . . Chen, Y. (2018). Organic and solution-processed tandem solar cells with 17.3% efficiency. Science,361(6407), 1094-1098. doi:10.1126/science.aat2612

2. Hachmann, J., Olivares-Amaya, R., Atahan-Evrenk, S., Amador-Bedolla, C., Sánchez-Carrera, R. S., Gold-Parker, A., . . . Aspuru-Guzik, A. (2011). The Harvard Clean Energy Project: Large-Scale Computational Screening and Design of Organic Photovoltaics on the World Community Grid. J. Phys. Chem. Lett. The Journal of Physical Chemistry Letters, 2(17), 2241-2251. doi:10.1021/jz200866s

3. Scharber, M., Mühlbacher, D., Koppe, M., Denk, P., Waldauf, C., Heeger, A., & Brabec, C. (2006). Design Rules for Donors in Bulk-Heterojunction Solar Cells—Towards 10 % Energy-Conversion Efficiency. Advanced Materials, 18(6), 789-794. doi:10.1002/adma.200501717

4. Harrison, N. (2006, August 28). An Introduction to Density Functional Theory. Retrieved January 15, 2016, from https://www.ch.ic.ac.uk/harrison/Teaching/DFT_NATO.pdf

5. Laurent, A. D., & Jacquemin, D. (2013). TD-DFT benchmarks: A review. International Journal of Quantum Chemistry, 113(17), 2019-2039. doi:10.1002/qua.24438

6. Evenson, S. J., & Rasmussen, S. C. (2010). N-Acyldithieno [3, 2-b: 2', 3'-d] pyrroles: Second Generation Dithieno [3, 2-b: 2', 3'-d] pyrrole Building Blocks with Stabilized Energy Levels. Organic letters, 12(18), 4054-4057.

7. Selvaraju, S., Adhikari, S., Hopson, R. A., Dai, S., Rheingold, A. L., Borunda, M. F., & Nelson, T. L. (2016). Effects of structural variations on the optical and electronic properties of eumelanin-inspired small molecules. Journal of Materials Chemistry C, 4(18), 3995-3999. doi:10.1039/c5tc03982g

8. Velusamy, M., Thomas, J., Lin, J. T., Hsu, Y., & Ho, K. (2005). Organic Dyes Incorporating Low-Band-Gap Chromophores for Dye-Sensitized Solar Cells. Organic Letters, 7(10), 1-4. doi:0.1021/ol050417f

9. A. A., Lopez-Arroyo, L., De la Cruz, P., Oswald, F., Meyer, T. B., & Langa, F. (2012). Organic Dyes Incorporating Oligothienylenevinylene for Efficient Dye-Sensitized Solar Cells. Organic Letters, 14(22), 1-4. doi:10.1021/ol302738k

10. A. A., Lopez-Arroyo, L., De la Cruz, P., Oswald, F., Meyer, T. B., & Langa, F. (2012). Organic Dyes Incorporating Oligothienylenevinylene for Efficient Dye-Sensitized Solar Cells. Organic Letters, 14(22), 1-4. doi:10.1021/ol302738k

11. Ebata, H., Miyazaki, E., Yamamoto, T., & Takimiya, K. (2007). Synthesis, Properties, and Structures of Benzo[1,2-b:4,5-b¢]bis[b]benzothiophene and Benzo[1,2-b:4,5-b¢]bis[b]benzoselenophene. Organic Letters, 9(22), 1-4. doi:10.1021/ol701815j

12. Steinberger, S., Mishra, A., Reinold, E., Muller, C. M., Uhrich, C., Bauerle, M., & Bauerle, P. (2011). A-D-A-D-A-Type Oligothiophenes for Vacuum-Deposited Organic Solar Cells. Organic Letters, 13(1), 1-4. doi:10.1021/ol102603n

13. Qian, X., Zhu, Y., Song, J., Gao, X., & Zheng, J. (2013). New Donor-π-Acceptor Type Triazatruxene Derivatives for Highly Efficient Dye-Sensitized Solar Cells. Organic Letters, 15(23), 1-4. doi:10.1021/ol402931u

14. Aeschi, Y., Li, H., Cao, Z., Chen, S., Amacher, A., Bieri, N., . . . Liu, S. (2013). Directed Metalation Cascade To Access Highly Functionalized Thieno[2,3-f]benzofuran and Exploration as Building Blocks for Organic Electronics. Organic Letters, 15(21), 1-4.

15. Lin, L., Lu, C., Huang, W., Chen, Y., Lin, H., & Wong, K. (2011). New A-A-D-A-A-Type Electron Donors for Small Molecule Organic Solar Cells. Organic Letters, 13(18), 1-4. doi:10.1021/ol2021077

16. Qian, X., Zhu, Y., Song, J., Gao, X., & Zheng, J. (2013). New Donor-π-Acceptor Type Triazatruxene Derivatives for Highly Efficient Dye-Sensitized Solar Cells. Organic Letters, 15(23), 1-4. doi:10.1021/ol402931u

17. Sean, E. J., & Rasmussen, S. C. (2010). N-Acyldithieno[3,2-b:2',3'-d]pyrroles: Second Generation Dithieno[3,2-b:2',3'-d]pyrrole Building Blocks with Stabilized Energy Levels. Organic Letters, 12(18), 4054-4057. doi:10.1021/ol101647f

18. Zhang, G., & Musgrave, C. (2006). Comparison of DFT Methods for Molecular Orbital Eigenvalue Calculations. J. Phys. Chem. A The Journal of Physical Chemistry A, 1554-1561.

19. Hanwell, M. D., Curtis, D. E., Lonie, D. C., Vandermeersch, T., Zurek, E., & Hutchison, G. R. (2012). Avogadro: An advanced semantic chemical editor, visualization, and analysis platform. J. Cheminformatics, 4(1), 17

20. Castro, A., Rubio, A., Rozzi, C. A., Lorenzen, F., Appel, H., Oliveira, M., Strubbe, D. A. (2014, April 03). The Octopus Manual Version 8.3.0. Retrieved from http://www.tddft.org/programs/octopus/wiki/index.php/The_Octopus_Manual

21. Perdew, J. P., & Yue, W. (1989). Erratum: Accurate and simple density functional for the electronic exchange energy: Generalized gradient approximation. Physical Review B, 40(5), 3399-3399. doi:10.1103/physrevb.40.3399

22. Giannozzi, P., Baroni, S., Bonini, N., Calandra, M., Car, R., Cavazzoni, C., ... & Dal Corso, A. (2009). QUANTUM ESPRESSO: a modular and open-source software project for quantum simulations of materials. J. Phys. Cond. Matt., 21(39), 395502.

23. Laurent, A. D., & Jacquemin, D. (2013). TD-DFT benchmarks: A review. International Journal of Quantum Chemistry, 113(17), 2019-2039. doi:10.1002/qua.24438

24. Python 3.7.0 documentation. (n.d.). Retrieved from https://docs.python.org/3/

Attachment 1: Octopus input file sample

#GEOMETRY OPTIMIZATION inp FOR OCTOPUS 7.2

```
#-------------------------------------------------------------------
#GENERAL PARAMETERS


CalculationMode = go
fromScratch = yes
UnitsOutput = eV_angstrom




EigenSolver = rmmdiis
ExtraStates = 4
ConvRelDens = 2e-6
SymmetriesCompute=no
MaximumIter = 500

GOMethod = fire
GOFireMass = 0.01
ExperimentalFeatures = yes


#----------------------------------------------------------------------
#BOX SHAPE AND SPACING

BoxShape = parallelepiped
Spacing = .25*angstrom
%Lsize
16*angstrom | 12*angstrom | 12*angstrom
%


#-----------------------------------------------------------------------
#SPECIES

%Species
          'C' | species_pseudo | file | 'C.psf' | mass | 12.011
          'H' | species_pseudo | file | 'H.psf' | mass | 1.0079
          'O' | species_pseudo | file | 'O.psf' | mass | 15.9994
          'N' | species_pseudo | file | 'N.psf' | mass | 14.00674
#         'S' | species_pseudo | file |'S.psf' | mass | 32.066
#         'F' | species_pseudo | file |'F.psf' | mass | 18.9984032 | lmax | 0 | lloc | 0
#         'Br' | species_pseudo | file | 'Br.UPF' | mass | 79.904
#         'Se' | species_pseudo | file | 'Se.psf' | mass | 78.96 | lmax | 1 | lloc | 1
#         'Si' | species_pseudo | file |'Si.psf' | mass | 28.0855
%


#-----------------------------------------------------------------------
#INPUT COORDINATES

UnitsXYZFiles = angstrom_units
XYZCoordinates = 'last.xyz'
```

Attachment 2: Quantum Espresso input file sample

```
&CONTROL
 calculation = 'relax',
 prefix = '01_M5_1a',
 wf_collect = .true.
 forc_conv_thr = 0.00050,
 tstress = .true.
 tprnfor = .true.
 pseudo_dir='/project01/borundagroup/solar/pseudos/'
 outdir = 'tmp/',
/
&system
 ibrav = 8,
 a = 25,
 b = 21,
 c = 15,
 ntyp = 9,
 nat = 18,
 ecutwfc = 55.0,
 ecutrho = 220.0,
 occupations = "smearing",
 smearing = "m-p",
 degauss = 0.05,
/
&electrons
 mixing_beta = 0.2,
 conv_thr = 1.0d-6
/
&IONS
/
ATOMIC_SPECIES
C          12.0107      C-PZ.UPF
H          1.0079                H-PZ.UPF
O          15.9994               O-PZ.UPF
N          14.00674     N-PZ.UPF
S          32.066                S-PZ.UPF
F          18.9984032   F-PZ.UPF
Br         79.904                Br-PZ.UPF
Se         78.96                 Se-PZ.UPF
Si         28.0855      Si-PZ.UPF
ATOMIC_POSITIONS (angstrom)
    H         -0.332497   2.490436   0.000000
    C         -0.187270   1.408122  -0.000000
    C          1.093599   0.870362   0.000000
    C          1.258216  -0.540206  -0.000000
    C          0.187270  -1.408122  -0.000000
    H          0.332497  -2.490436  -0.000000
    C         -1.093599  -0.870362   0.000000
    C         -1.258216   0.540206  -0.000000
    C         -2.345881  -1.541475  -0.000000
    C         -3.396791  -0.689425  -0.000000
    H         -2.452396  -2.626491   0.000000
    S         -2.929805   0.959074  -0.000000
    H         -4.454109  -0.943603   0.000000
    S          2.929805  -0.959074  -0.000000
    C          3.396791   0.689425   0.000000
    C          2.345881   1.541475  -0.000000
    H          2.452396   2.626491   0.000000
    H          4.454109   0.943603  -0.000000
K_POINTS {automatic}
1 1 1 0 0 0
```